Hybrid Microgels with ZnS Inclusions

Andrij Pich,*,† Jessica Hain,† Yan Lu,† Volodymyr Boyko,‡ Yuri Prots,§ and Hans-Juergen Adler†

Institute of Macromolecular Chemistry and Textile Chemistry, Dresden University of Technology, D-01062 Dresden, Germany; Institute of Physical Chemistry and Electrochemistry, Dresden University of Technology, D-01062 Dresden, Germany; and Max Planck Institute of Chemical Physics of Solid Materials, D-01187 Dresden, Germany

Received March 11, 2005; Revised Manuscript Received May 3, 2005

ABSTRACT: We report on a preparation of hybrid microgels filled with ZnS inclusions. Temperature-sensitive poly(*N*-vinylcaprolactam-*co*-acetoacetoxyethyl methacrylate) (VCL/AAEM) microgels have been used as containers for deposition of ZnS by reaction of zinc acetate and thioacetamide under ultrasonic agitation. ZnS was deposited directly into microgels, leading to formation of composite particles which exhibit temperature-sensitive properties, high ZnS contents, and excellent colloidal stability. The influence of ZnS load on microgel size, morphology, swelling−deswelling behavior, and stability is discussed. Hybrid particles contain up to 20 wt % of ZnS, and particle stability decreases with increase of inorganic filler content. Detailed microscopy investigations confirm incorporation of ZnS nanoparticles into microgel network. The possibility of self-assembly of hybrid particles on different surfaces was studied. It has been found that microgels filled with ZnS can form organized particle arrays after water evaporation.

Introduction

Nanocoating techniques lead to the formation of novel inorganic−organic functional hybrid materials with tailored properties that depend on the combination of components employed in the fabrication process. Materials for specific applications in catalysis, electronics, and biomaterials engineering can be designed by careful selection of the components and template morphology. The majority of the templates used for preparation of hybrid materials can be produced at the present moment with monodisperse size (colloid particles) or of controlled morphology (membrane pore structure, crosslinking density of gel, etc.).

The interest in microgels as polymeric templates has grown rapidly over the past 20 years because of their easy preparation and their potential uses in many industrial applications. Microgels are currently being investigated for their use as drug delivery systems, in chromatographic separation technology, as catalyst media, etc.[1−3] If to compare with dendrimers[4] or star block copolymers,[5] polymer microgels can be easily synthesized, and different possibilities for incorporation of reactive groups are available. Additionally, the size of the microgels can be effectively varied from nano- to microscale by choosing the proper polymerization technique. It has been also realized by numerous scientists that microgels can be excellent microreactors for preparation of different inorganic materials. The reason for this is the network structure of microgels which can be used for preparation of semiconductor, metal, or magnetic nanoparticles.[6]

Zink sulfide (ZnS) is widely used in numerous technical systems such as paints,[7] solar cells,[8] IR windows,[9] etc. Formation of ZnS colloids with defined size can be achieved by precipitation and aggregation methods.[10,11] There are a large number of reports in the literature about synthesis and characterization of ZnS nanoparticles in aqueous medium.[12−18] Preparation of composite materials on ZnS basis can be divided into two parts, namely (a) composite materials with polymers and (b) well-defined particles. Polymeric particles containing ZnS have been prepared by utilizing microgel,[19] SiO_2,[20] or polystyrene[21] particles as templates. Bai et al.[19] reported synthesis of composite microspheres containing ZnS with patterned structures by using poly(*N*-isopropylacrylamide-*co*-methacrylic acid) microgels as templates. It has been reported that the surface structures of obtained particles depend strongly on the ratio of the metal sulfide to the template, indicating that microgel network plays role of confinement and guidance of the precipitation of ZnS. Velikov et al.[20] used silica particles for deposition of ZnS or vice versa for preparation of core−shell structures. Formation of well-defined ZnS layers on SiO_2 surface was achieved, and hollow particles were obtained after removal of silica core. Deposition of ZnS on the surface of polystyrene particles modified with carboxylic groups has been reported by Breen et al.[21] The ZnS deposition process on the particle surface leads to formation of 70−80 nm thick uniform zinc sulfide layers.

In present paper we report on preparation of hybrid microgels containing polymeric matrix filled with ZnS nanoinclusions. Our aim was to explore the preparation of ZnS nanoparticles in the presence of polymeric microgels by the ultrasonication method and obtain particles which combine thermosensitivity and typical physicochemical properties of zink sulfide.

The motivation of the present investigations is preparation of multisensitive composite particles which can combine attractive physicochemical properties of polymers and inorganic materials. Novel temperature-sensitive poly(*N*-vinylcaprolactam-*co*-acetoacetoxyethyl methacrylate) (VCL/AAEM) microgels have been selected as sub-microcontainers for deposition of ZnS

† Institute of Macromolecular Chemistry and Textile Chemistry, Dresden University of Technology.
‡ Institute of Physical Chemistry and Electrochemistry, Dresden University of Technology.
§ Max Planck Institute of Chemical Physics of Solid Materials.
* Corresponding author: e-mail andrij.pich@chemie.tu-dresden.de.

10.1021/ma0505272 CCC: $30.25
Published on Web 06/23/2005

nanoparticles. It is expected that by controlled deposition of inorganic nanoparticles into microgels it could be possible to preserve the most important features of these polymeric particles, namely *T* sensitivity, colloidal stability, etc. Additionally, well-controlled reaction process should allow flexible incorporation of different amounts of ZnS nanoparticles into polymeric networks and their properties (size, polydispersity, location in the microgel, etc.) can be also tuned. For this aim preparation of ZnS nanoparticles and their incorporation into microgels by means of ultrasound seems to be the attractive technique, since it allows preparation of semiconductor particles of nanometer size and continuous agitation prevents aggregation of inorganic nanoparicles and probably better distribution in microgel network. It is expected that obtained hybrid microgels should have large application potential in different fields of material science. One of the most important applications for such hybrid microgels is photocatalysis. Such particles can act as smart catalyst where ZnS nanoparticles are responsible for generation of electron−hole pairs by irradiation with light of certain wavelength providing possibilities for oxidation−reduction processes. Simultaneously, porous microgel matrix can provide suitable environment for diffusion and adsorbion of different organic molecules. Therefore, obtained hybrid microgels can be used for UV-mediated synthesis in aqueous or organic phases or destruction of organic molecules in wastewater.

Experimental Section

Materials. Acetoacetoxyethyl methacrylate (AAEM) was obtained from Aldrich and purified by conventional methods and then distilled under vacuum. *N*-Vinylcaprolactam (VCL) was obtained from Aldrich and purified by distillation. The initiator 2,2′-azobis(2-methylpropyonamidine) dihydrochloride (AMPA) was obtained from Aldrich and used as received. The cross-linker *N,N*′-methylenebis(acrylamide) (BIS) from Aldrich was used without further purification. Zink acetate (ZnAc) and thioacetamide (TAA) were received from Aldrich and used as commercially available. Distilled water was employed as polymerization medium.

Synthesis of VCL/AAEM Microgels. Detailed information about synthesis of VCL/AAEM microgels has been reported in ref 26. Appropriate amounts of AAEM (0.16 g), VCL (1.98 g), and cross-linker (3 mol %) were added in 145 mL deionizer water. Double-wall glass reactor equipped with stirrer and reflux condenser was purged with nitrogen. Solution of the monomers was placed into reactor and stirred for 1 h at 70 °C with purging with nitrogen. After that the 5 mL water solution of initiator (5 g/L) was added under continuous stirring. Reaction was carried out for 8 h. Microgel dispersion was purified by dialysis with the Millipore dialysis system (cellulose membrane, MWCO 100 000).

Synthesis of Hybrid Microgels. Preparation of ZnS-containing composite microgels has been performed by method described by Breen et al.[21] VCL/AAEM dispersion was placed into a glass vessel; ZnAc and TAA solution was added (ZnAc:TAA molar ratio was 1:1). Reaction mixture was ultrasonically agitated by titanium tip immersed directly into the solution (Branson Sonifier, power output 90 W in pulsed operation regime 20%). During ultrasonic agitation reaction mixture was cooled to 5 °C. After 6 h formed composite particles were removed from reaction vessel and cleaned by precipitation to remove all byproducts.

Characterization. *Particle Size Analysis*. A commercial laser light scattering (LLS) spectrometer (ALV/DLS/SLS-5000) equipped with an ALV-5000/EPP multiple digital time correlator and laser goniometer system ALV/CGS-8F S/N 025 was used with a helium−neon laser (Uniphase 1145P, output power of 22 mW and wavelength of 632.8 nm) as the light source. With static LLS it is possible to obtain both the weight-average molar mass (M_w) and the *z*-average radius of gyration R_g of scattering objects in an extremely dilute solution because the Rayleigh ratio $R(q)$ is dependent on the scattering vector q as

$$\frac{Kc}{R(q)} = \frac{1}{M_w}\left(1 + \frac{(qR_g)^2}{3}\right) + 2A_2c \tag{1}$$

where $K = 4\pi^2n^2(\mathrm{d}n/\mathrm{d}c)^2/(N_A\lambda_0^4)$ and $q = (4\pi n\lambda_0)\sin(\theta/2)$ with n, N_A, λ_0, θ, and c being the solvent refractive index, Avogadro's number, the wavelength of the incident light in a vacuum, the scattering angle, and concentration, respectively.

In dynamic LLS, the intensity−intensity time correlation function $g_2(q,t)$ in the self-beating mode was measured and can be expressed by the Siegert relation

$$g_2(q,t) = A(1 + \beta|g_1(q,t)|^2) \tag{2}$$

where t is the decay time, A is a measured baseline, β is the coherence factor, and $g_1(q,t)$ is the normalized first-order electric field time correlation function, and $g_1(q,t)$ is related to the measured relaxation rate Γ:

$$g_1(q,t) = \int G(\Gamma)\exp(-\Gamma t)\,\mathrm{d}\Gamma \tag{3}$$

A line-width distribution $G(\Gamma)$ can be obtained from the Laplace inversion of $g_1(t)$ (CONTIN procedure).[10] For a pure diffusive relaxation, Γ is related to the translational diffusion coefficient D at $q \to 0$ and $c \to 0$ by

$$D = \Gamma/q^2 \tag{4}$$

or a hydrodynamic radius R_h given by

$$R_h = k_BT/(6\pi\eta D) \tag{5}$$

with q, k_B, T, and η being the scattering vector, the Boltzmann constant, absolute temperature, and solvent viscosity, respectively. All DLS experiments were carried out at angles θ = 30°−140°. The sample in a 10 mm test tube was immersed in a toluene bath and thermostated within an error of ±0.1 °C. Typically, three measurements were performed for determination of the radius of gyration and five for the hydrodynamic radius. Accuracy of measurements for radius of gyration is ±6% and for hydrodynamic radius is ±3%.

Stability Measurements. Stability measurements were performed with separation analyzer LUMiFuge 114 (L.U.M. GmbH, Germany). Measurements were made in glass tubes at acceleration velocities from 500 to 3000 rpm. The slope of sedimentation curves was used to calculate the sedimentation velocity and to get information about stability of the samples.

Scanning Electron Microscopy (SEM). SEM images were taken with a Gemini microscope (Zeiss, Germany). Samples were prepared in the following manner. Microgel dispersions were diluted with deionized water, dropped onto cleaned support, and dried at room temperature or 45 °C. Samples were coated with thin Pd layer to increase the contrast and quality of the images. Pictures were taken at voltage of 4 kV.

Atomic Force Microscopy (AFM). AFM images were obtained with a Dimension 3100 scanning probe microscope (SPM, Digital Instruments, Santa Barbara, CA) operating in tapping mode with a drive frequency 257 kHz. Samples were prepared by casting 4−5 drops of dispersion onto freshly cleaved quartz plates, and they were allowed to dry.

Transmision Electron Microscopy (TEM). TEM images were obtained with a Zeiss Omega 912 at voltage 10 kV. Diluted microgel dispersions were placed onto Au nets and dried at room temperature.

Thermogravimetrical Analysis (TGA). To determine the ZnS content in composite particles, the TGA 7 Perkin-Elmer instrument (Pyris-Software version 3.51) was used. Before measurement samples were dried in a vacuum for ca. 48 h.

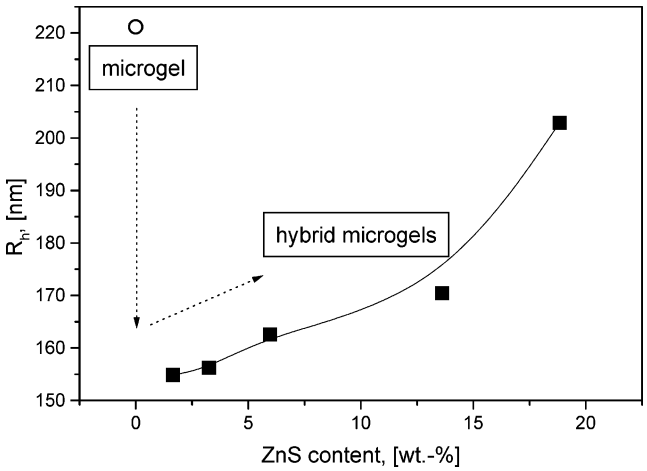

Figure 1. Hydrodynamic radii of microgel and hybrid microgels containing different ZnS amounts (measurements performed at 22 °C).

Table 1. Ingredients Used for Preparation of VCL/AAEM/ZnS Particles

sample	microgel [g]	ZnAc [g]	TAA [g]	ZnS [wt %]
1	0.564	0.127	0.044	1.66
2	0.460	0.622	0.231	3.26
3	0.459	0.828	0.284	5.97
4	0.321	0.724	0.248	13.62
5	0.325	1.466	0.502	18.84

Samples were analyzed in closed aluminum cups in the temperature range 25−600 °C (heating rate 5 K/min in a nitrogen atmosphere).

Elecrophoretic Mobility Measurements. Elecrophoretic mobility measurements have been performed with Zetasizer 2000, Malwern Instruments. pH was adjusted by addition of 0.01 M NaOH or 0.01 M HCl. The average value of at least 10 measurements was adopted as electrophoretic mobility (or transformed into ξ potential) at a given pH value.

UV Measurements. Thin transparent films have been prepared on quartz plates and investigated with a Perkin-Elmer UV−vis spectrometer Lambda 45.

XRD Measurements. XRD spectra of the hybrid microgels were recorded with a Siemens P5005 powder X-ray diffractometer equipped with a Cu Kα (wavelength 1.540 Å) radiation source using the Diffracplus software.

Results and Discussion

Synthesis of Hybrid Microgels. A sequence of hybrid particles has been prepared by using VCL/AAEM microgel as a template and varying the ZnS content deposited into polymeric network. Table 1 summarizes the amounts of ingredients used for preparation of hybrid particles as well as the finally measured ZnS content. The maximal ZnS content deposited into polymeric microgels was close to 20 wt %.

During ZnS synthesis the reaction mixture was cooled to 5 °C to keep VCL/AAEM particles in swollen state. This can ensure more effective incorporation of semiconductor nanoparticles into microgels due to better conditions for diffusion of reactants as well as formed ZnS clusters.

Characterization of Obtained Hybrid Particles. *Particle Size and Colloidal Stability.* Incorporation of ZnS into microgels has a strong influence on particle size of obtained hybrid particles. Figure 1 shows hydrodynamic radii of microgel particles and hybrid particles prepared with different ZnS contents. It is interesting to note that incorporation of small ZnS amount into microgels leads to decrease of the particle radius from 220 to 155 nm. Further increase of ZnS content leads to continuous increase of particle dimensions. At highest ZnS load some discrete ZnS particles have been detected in the aqueous phase which indicates that maximal capacity of microgel as template has been reached.

Shrinkage of microgels after incorporation of small ZnS amounts can be explained by effective interactions of ZnS inclusions with the polymeric network. A similar effect has been observed in our previous work when microgels have been filled with polypyrrole[27,28] or magnetite.[25] The pH value of investigated dispersions was close to 6, and as will be shown later, ZnS particles possess nearly no charge in this pH range. This can lead to conclusion that the interaction of ZnS particles with polymeric network possess some hydrophobic character, which influences probably also the swelling degree of microgel in the aqueous phase. Increase of ZnS content can induce expansion of the microgel due to the incorporation of solid material which occupies the pores inside the particles and therefore prevents them from shrinkage.

Following above-mentioned considerations, incorporation of inorganic material into porous polymeric particles will increase particle density and influence colloidal stability of hybrid particles. The stability of hybrid microgels was investigated by sedimentation method developed by Lerche et al.[22]

In a special centrifuge an integrated optoelectronic sensor system allows spatial and temporal changes of light transmission during the rotation to be detected. In contrast to other approaches,[23] the local transmission is determined over the entire sample length simultaneously. Throughout the measurement, transmission profiles are recorded, and the sedimentation process can be depicted as a time course of the relative position of the boundary between supernatant and sediment (resolution better than 100 μm) or of the transmission averaged over the entire or a chosen part of the sample length. On the basis of obtained data the sedimentation constants, the packing density, etc., can be derived.

The experimental results from sedimentation centrifuge are summarized in Figure 2. Parts a and b of Figure 2 indicate that light transmission and sedimentation front position, respectively, increase with time, indicating that particles precipitate due to the action of centrifugal force. It is also clear that the two above-mentioned parameters possess different behavior for hybrid particles with different ZnS contents; namely, increase of inorganic filler content induces faster particle sedimentation at similar experimental conditions. From experimental data presented in Figure 2a,b sedimentation velocity was calculated for different samples (Figure 2c). It is clear that sedimentation velocity increases in linear order with increase of ZnS content. This leads to the conclusion that incorporation of inorganic material has a strong influence on colloidal stability of microgels, and probably at some critical ZnS value a microgel template will be not able to provide effective stabilization for hybrid particles.

Electrophoretic Mobility Measurements. Another important property of polymeric particles is their charge, which can be determined by electrophoretic mobility measurements. In present system we incorporate inorganic material into polymeric particles, and this modification can influence the charge of final hybrid particles. Electrophoretic measurements were performed at different pH values, and experimental results are sum-

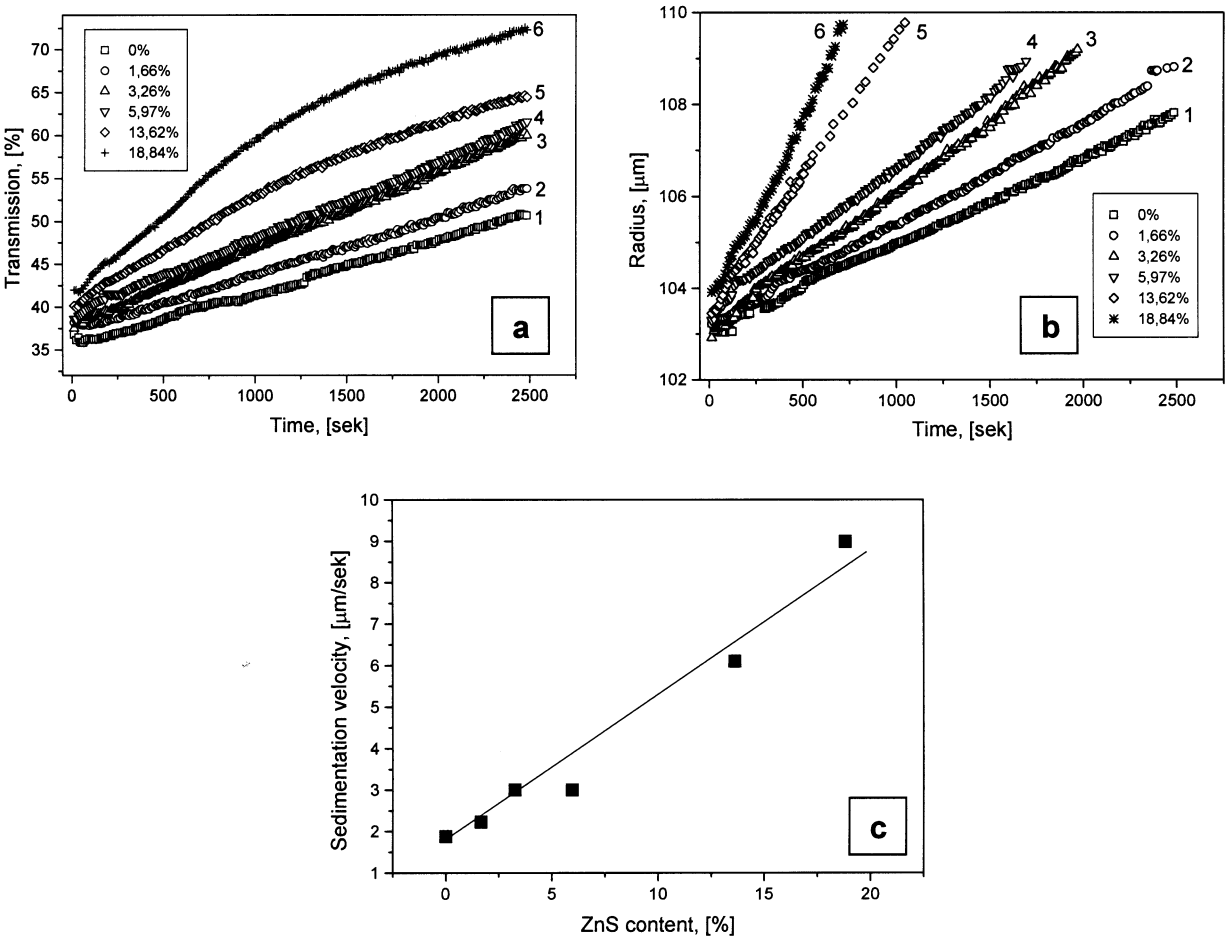

Figure 2. Transmission−time curves (a), sedimentation−time curves (b), and calculated sedimentation velocity data (c) for hybrid microgels with different ZnS contents (measurements performed at 3000 rpm).

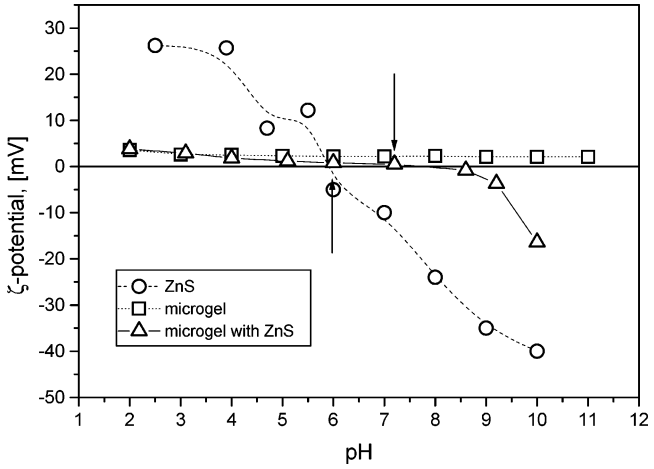

Figure 3. ξ-potential measurements for ZnS, microgel template, and hybrid particles (1.66 wt % ZnS) as a function of pH (measurements performed at 22 °C).

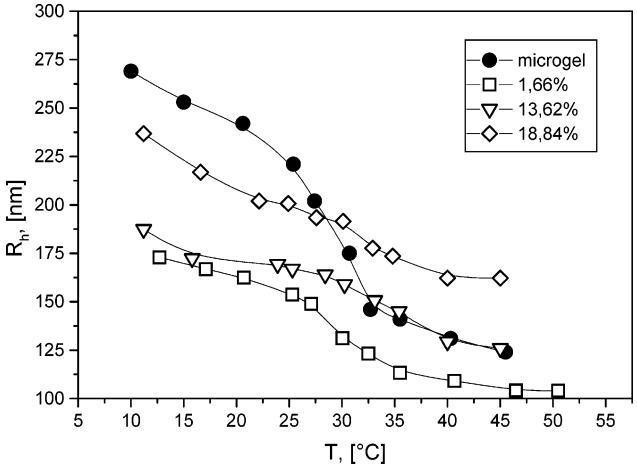

Figure 4. Hydrodynamic radii vs temperature for hybrid microgels with different ZnS contents.

marized in Figure 3. ZnS particles possess an isoelectrical point at pH = 5, and this result is in agreement with observations of other authors.[24] Microgel particles possess weak positive charge in all pH range due to the functional groups originating from cationic azo-initiator incorporated into polymer structure during polymerization process.[25]

Hybrid particles exhibit similar behavior to microgels in pH range from 2 to 7, but in the basic region particle charge changes to negative similar to ZnS particles. The isoelectrical point for hybrid particles was detected at pH = 7.5. A possible reason for such behavior is partial compensation of negative charges of ZnS by positive charges of microgel template.

Influence of the Temperature and pH on Particle Size. Another important feature of polymeric microgels used as templates in the present study is their thermosensitive character. In our previous studies[26−28] we showed that VCL/AAEM microgel particles possess core−shell structure due to fast consumption of the more reactive methacrylic monomer (AAEM). The PVCL-rich microgel shell exhibits a lower critical solution temper-

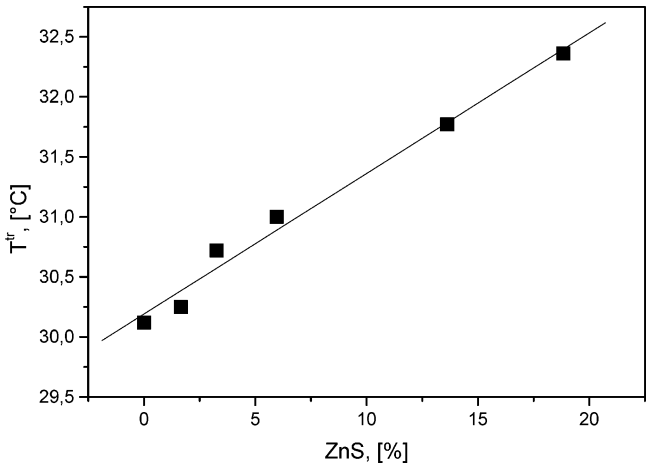

Figure 5. Transition temperature vs ZnS content for hybrid microgels.

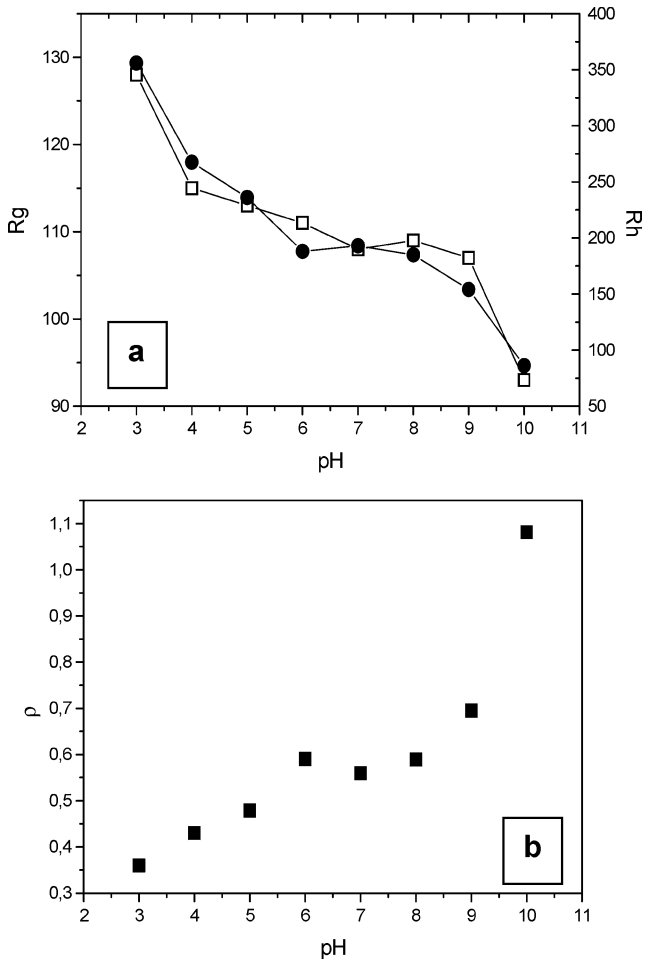

Figure 6. Hydrodynamic radii (R_h) (solid symbols) and radius of gyration (R_g) (open symbols) (a) and calculated ρ parameter ($\rho = R_g/R_h$) (b) for sample containing 1.66% ZnS.

ature (LCST) in aqueous solution, and this transition temperature was detected at ~30 °C in comparison to the reported 32 °C for pure PVCL. The AAEM-rich particle core is more hydrophobic and is less temperature sensitive if compared with the VCL-rich shell. VCL/AAEM microgel particles exhibit a fully reversible "soft−hard sphere" transition induced by collapse of the highly swollen VCL-rich shell during heating. To investigate the influence of ZnS inclusions on thermosensitivity of obtained particles, DLS measurements have been performed at different temperatures. Figure 4

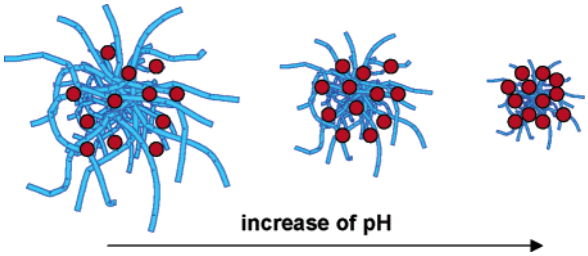

Figure 7. Schematic representation of possible interactions inside hybrid microgels.

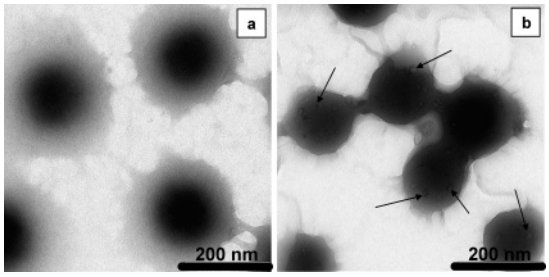

Figure 8. TEM images of VCL/AAEM microgels (a) and microgel filled with 13.62% ZnS (b).

shows experimental results of hydrodynamic radii for several hybrid particles determined at different temperatures.

It is obvious from Figure 4 that incorporation of ZnS into microgel particles changes considerably the behavior of hydrodynamic radius at different temperatures. Incorporation of a very small ZnS amount (1.66%) leads to much smaller particle shrinkage at high temperatures. As the ZnS amount in microgels increases, the experimental data are shifted to higher R_h values. However, experimental results presented in Figure 4 let us conclude that the obtained hybrid particles have thermosensitive character provided by the VCL/AAEM microgel matrix.

It is also noticeable that there is some influence of ZnS inclusions on transition point of measured curves in Figure 5. The volume transition temperature is shifted to higher values in linear order with ZnS content.

This effect is definitely induced by ZnS nanoparticles which can influence LCST of PVCL chains of microgel by some specific interactions. But the origin of these interactions is not clear because in the present case ZnS nanoparticles should possess more or less neutral charge (pH = 6), so it can be expected that hydrophobic attraction forces are dominating. In this case it is logical to expect some decrease of transition temperature. It should be also taken into account that the data presented in Figure 5 have been obtained by differentiation of the curves from temperature-dependent DLS measurements, and because of the broad transition which is characteristic for all samples, the exact value of the transition temperature is difficult to determine. Some additional measurements are necessary to prove and explain the effects discussed above.

On the basis of electrophoretic mobility measurements presented in Figure 3, one can assume that dimensions of hybrid microgels can be also influenced by the pH value of the aqueous solution. Let us consider that our hybrid particle consists out of polymeric matrix which possess some weak positive charges and inorganic filler which is able to change the charge from positive to negative. Then it is possible to assume that repulsion

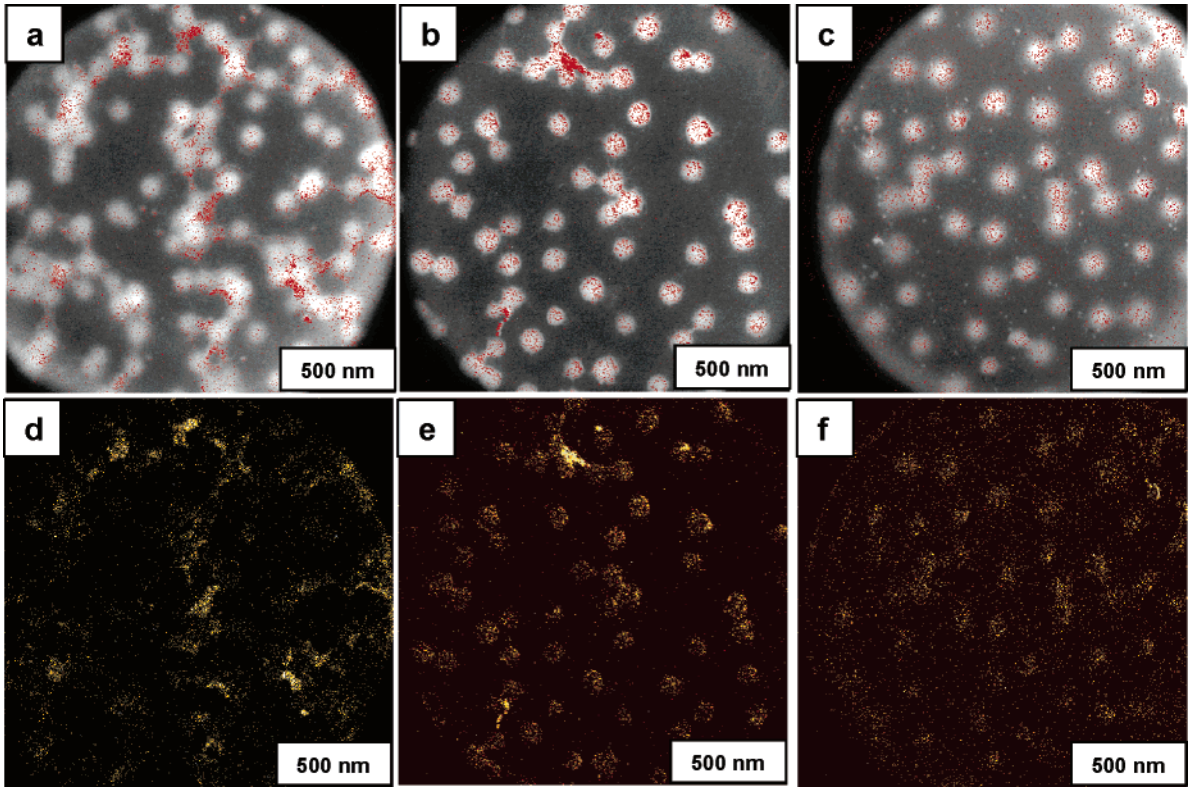

Figure 9. Elemental mapping images of microgels containing 3.26% (a, d), 13.62% (b, e), and 18.84% (c, f) ZnS.

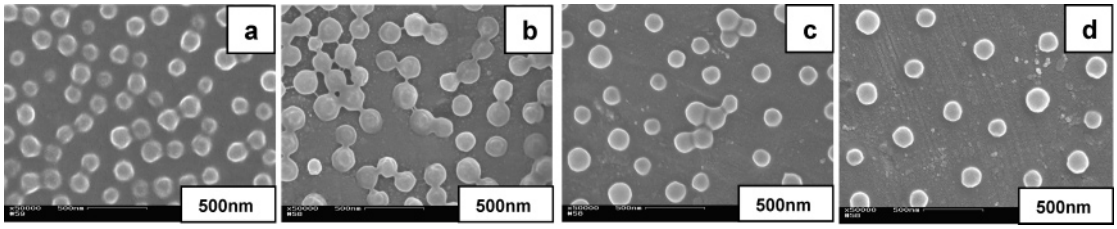

Figure 10. SEM images of microgels prepared at different ZnS contents: microgel particles (a), 1.66% (b), 3.26% (c), and 5.97% (d).

or attraction interactions inside of microgels will change particle dimensions if the temperature is constant. The combination of static and dynamic light scattering was used to check the influence of the pH on hydrodynamic radius and radius of gyration at temperature when microgels are in the swollen state (10 °C). Figure 6a shows the experimental results which indicate that the general trend is decrease of both R_h and R_g with increasing pH value of aqueous solution.

It is interesting to note that both R_h and R_g decrease continuously up to pH = 6, and then a plateau is reached with next rapid decrease after pH value 7.5. As was shown earlier, at these pH values isoelectrical point has been detected for ZnS particles (pH = 6) and hybrid microgel (pH = 7.5).

If we consider electrophoretic mobility and light scattering measurements, then such effects can be explained by considering the possible interactions inside hybrid microgel (Figure 7). In the acidic region the microgel template possesses weak positive charges, and ZnS nanoinclusions should be also positively charged. So, in this area we can expect some repulsion forces between the matrix and ZnS as well as between ZnS particles. If the pH value shifted from 2 to 6, the charge of ZnS particles becomes smaller and less repulsive interactions can be expected, so microgel shrinks gradually. At pH = 6 (isoelectrical point of ZnS) we can expect some attractive forces between polymeric matrix and inorganic particles based mostly on hydrophobic interactions. As soon as pH is higher than 7 and ZnS particles are negatively charged, there could be strong electrostatic attraction between positively charged polymeric matrix and inorganic filler, and this is indeed the case because both R_h and R_g continue to decrease in this pH range (Figure 6a). Calculated ρ-parameter values presented in Figure 6b confirm the above-mentioned considerations showing the transition from microgel (ρ = 0,4−0,5) to hard spherical particles (ρ = 0,75) as the pH value increases.

Particle Morphology. The morphology of hybrid particles was investigated by different microscopy techniques. TEM images of microgels indicate clearly the presence of ZnS inclusions (see arrows) in hybrid particles (Figure 8b) distributed homogeneously in the polymeric network. A reference image presented in Figure 8a can be used where microgels containing no ZnS are shown.

TEM investigations allowed obtaining elemental mapping images (EMI) for hybrid particles prepared with different ZnS contents. Results are presented in Figure 9a−c for microgels containing 3.26%, 13.62%, and 18.84% ZnS. In this case the light areas are polymeric

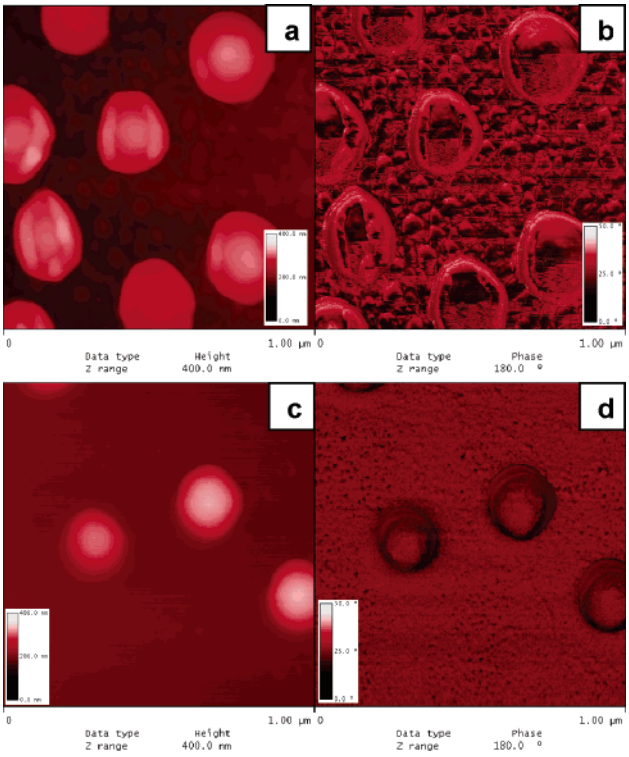

Figure 11. AFM images of microgel (a, b) and hybrid microgel with 18.84% ZnS (c, d) (left: topography image, window size 1 μm, height 0−400 nm; right: phase image, window size 1 μm, angle 0−50°).

particles, and areas enriched with Zn appear as red dots. Figure 9d−f presents inverse images of similar samples where only Zn areas are visible as light dots. One can see that increase of Zn signal in EMI images with increasing ZnS content in hybrid microgels. At low ZnS content (Figure 9a) one can find large areas where the Zn signal is very strong. This effect is present due to the migration of ZnS inclusions during drying and the partial film formation process which leads to some local phase separation. Particles with higher ZnS contents show less tendency to film formation; therefore, such effects are not present. Figure 9c shows also that there are ZnS particles which are not included into polymer matrix and remain beside composite particles. This correlates with light scattering measurements discussed before.

Figure 10 shows SEM images of microgel particles containing different ZnS amounts. In Figure 10a microgel particles containing no inorganic filler stick together and form a layerlike structures due to the partial fusion of less cross-linked shells. Increase of ZnS amount in microgels reduces considerably the film-formation properties of composite particles, and at higher ZnS loads separate particles can be found on the substrate.

AFM images of microgel particles are presented in Figure 11. Comparing height images in Figure 11a,c, one can see that particle size of microgels is reduced considerably after incorporation of ZnS. The phase image shown in Figure 11b indicates that microgels are highly deformed during the drying process; contrary hybrid particles remain spherical as is presented in Figure 11d. Particle flattering after deposition on solid substrate was also detected by height profiles obtained from line scans (Figure 12a,b).

It can be concluded that incorporation of ZnS into microgels reduces the size of composite particles which correlates with DLS measurements presented in Figure 1. Additionally, incorporation of inorganic particles provides some shape stability for composites and particles remain spherical after drying (see Figure 11c,d and Figure 12c,d). These observations are also in agreement with SEM measurements. However, both

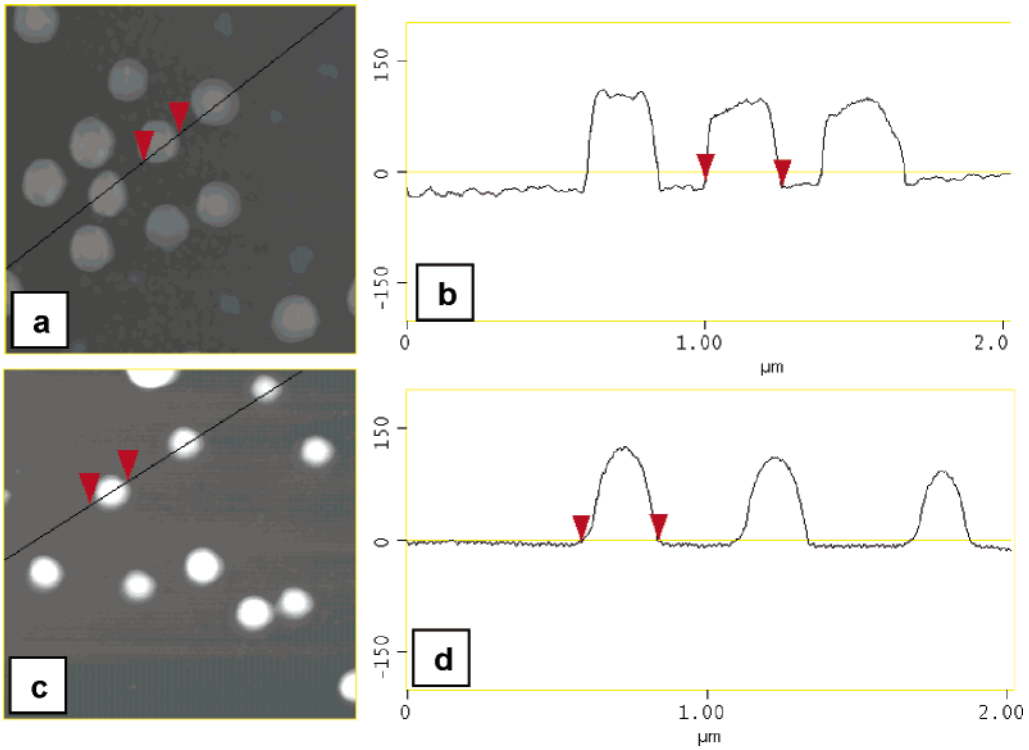

Figure 12. AFM images of microgel (a) and hybrid microgel with 18.84% ZnS (c) with corresponding height profiles (b, d) obtained from line scans showed as black lines in images a and c (window size for images a and c: 2 μm).

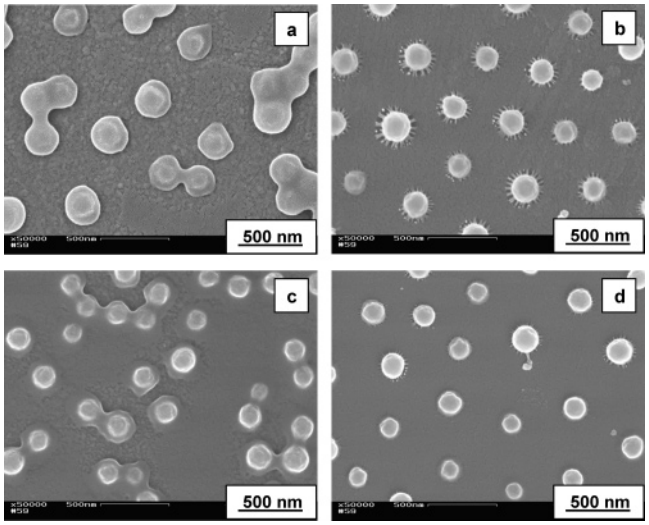

Figure 13. SEM images of microgels (a, c) and hybrid microgels containing 13.62% ZnS (b, d) deposited on glass (a, b: drying at room temperature; c, d: drying at 45 °C).

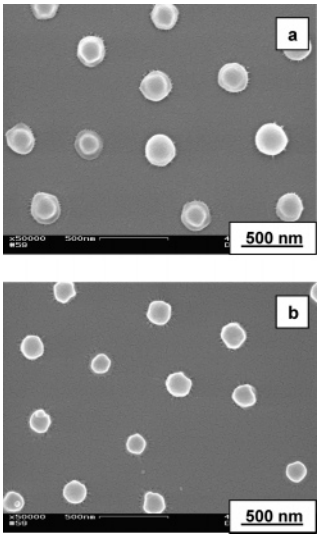

Figure 14. SEM images of hybrid microgels containing 13.62% ZnS: solution pH = 2 (a); solution pH = 11 (b) (substrate: silicium).

height and phase AFM images presented in Figure 11c,d do not show clearly ZnS nanoparticles embedded into the microgel network.

Detailed electron microscopy investigations confirmed that hybrid microgel particles possess ability to form organized arrays on different substrates during drying process. This effect can be observed if highly diluted microgel dispersions dry on different substrates. SEM images of microgels deposited on glass surface are shown in Figure 13. It is obvious that VCL/AAEM microgels have affinity to stick to each other and form clusters during drying. Especially this effect is pronounced if the drying temperature is 45 °C (compare parts a and c of Figure 13). Contrarily, hybrid microgels exhibit some tendency to form ordered patterns where particles are well separated and build a kind of lattice on the substrate. Even drying at 45 °C did not cause particles to form aggregates, and particles are slightly smaller in this case (compare parts b and d of Figure 13). This effect can be explained by effective electrostatic repulsion between particles provided by ZnS domains, so that during water evaporation particles remain a

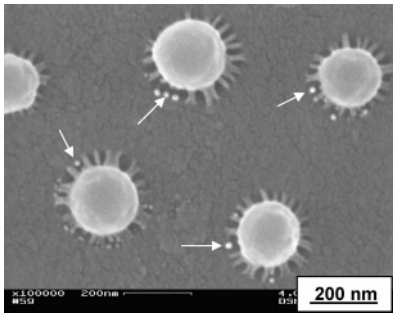

Figure 15. SEM image of hybrid microgels containing 13.62% ZnS (substrate: glass).

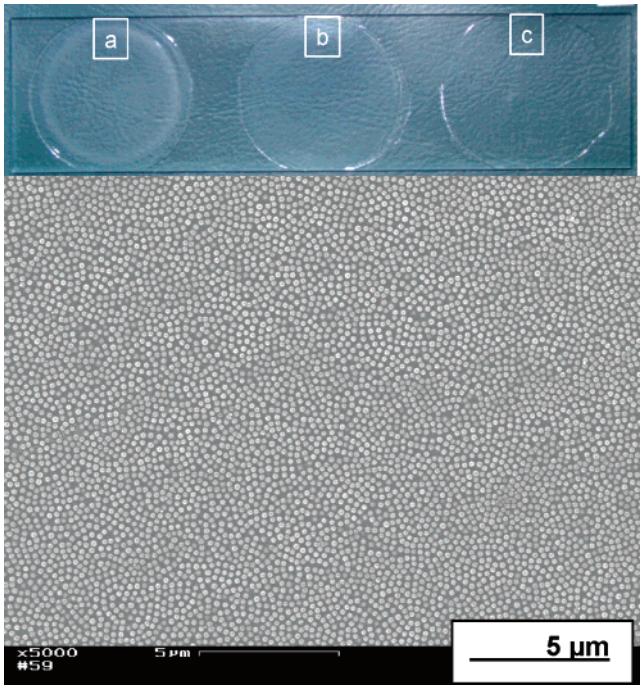

Figure 16. Photographs of films prepared from hybrid microgels with different ZnS contents: 1.66% (a), 5.97% (b), and 18.84% (c) (bottom image: SEM micrograph of sample c).

certain distance from each other. This interesting feature can provide possibilities for preparation of patterned structures on different surfaces where the interparticle distance or particle size can be varied by changing the sample preparation conditions.

Another example is shown in Figure 14 where hybrid microgels were deposited onto the substrate from solutions with different pH values. It is clearly seen that in the case of pH = 11 particles are considerably smaller, which correlates with the light scattering measurements discussed above.

It is interesting to have more insight into the structure of hybrid microgels. Figure 15 shows microgel particles at higher magnification.

It is clearly visible that during the drying process types of arms or fibers have been formed from collapsed polymeric chains which connect every microgel particle to the substrate. In some cases even separate ZnS particles are visible (see arrows) which were probably released during shrinkage of the microgel core and increasing of spacing between polymeric arms. The formation of microgel arrays should be investigated in the future also on different substrates to optimize the deposition process and create interesting organized structures.

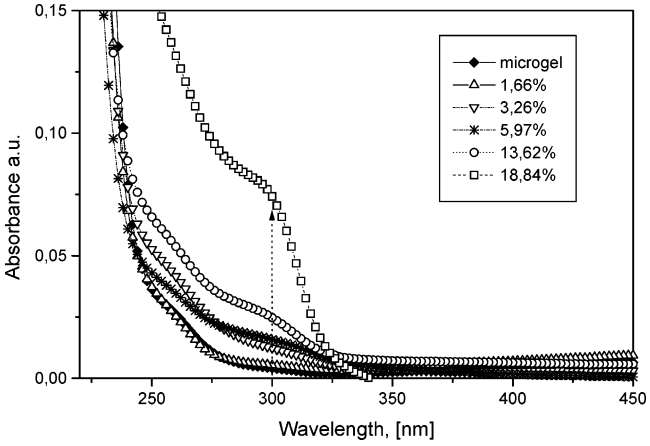

Figure 17. UV−vis spectra of VCL/AAEM/ZnS particles with different ZnS contents.

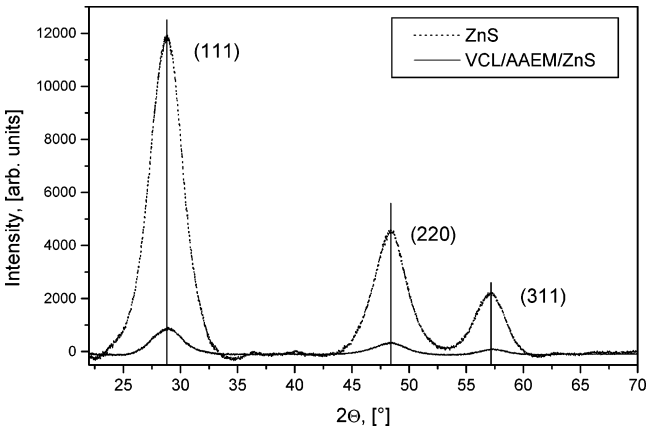

Figure 18. X-ray powder diffraction spectrum of ZnS and VCL/AAEM/ZnS particles (18.84% ZnS).

It has been found that controlled drying of concentrated microgel dispersions leads to formation of thick optically transparent films with excellent quality. Figure 16a−c shows photos of such films prepared on the glass surface by drying at room temperature.

One can see that there is no influence of the ZnS content on the film quality, and in all cases no visible phase separation can be detected. A closer look at the morphology of such coating with microscope (Figure 16, bottom) clearly indicated organized arrangement of hybrid particles into special arrays where white dots represent microgel cores with ZnS and flexible shells form a continuous phase.

Bulk Properties of Hybrid Particles. UV/vis measurements have been performed to characterize the optical properties of the composite microgel particles. As shown in Figure 17, the sample prepared at smallest ZnS content showed an onset of absorption at ca. 350 nm. Increase of the ZnS content in the samples leads to the gradual shift of the onset absorption to higher wavelength. It is known that the UV/vis onset absorption of semiconductor particles is attributed to the band-gap absorption, and as expected, it should be red-shifted if ZnS particles grow in size. A similar effect was reported by Du et al.[29] for polystyrene particles with CdS shells.

The XRD pattern of ZnS shows the presence of three peaks (Figure 18), corresponding to the zinc blende crystal structure. Those diffraction peaks correspond to the (111), (220), and (311) planes of the cubic crystalline ZnS. This sample was prepared at similar conditions as hybrid particles but without microgel particles in the reaction mixture.

The XRD pattern of hybrid particles shows also three weak broad peaks which have similar position as pure ZnS. The presence of weak XRD signals in VCL/AAEM/ZnS sample can be attributed to the partial crystalline nature of ZnS and/or to the relatively small amount of ZnS (18.84%).

Conclusions

In present paper we report on preparation of hybrid microgels which consist of polymeric matrix and ZnS nanoinclusions. Incorporation of ZnS was performed by means of ultrasonic treatment of zinc acetate and thioacetamide in the presence of preformed VCL/AAEM microgel particles. In this way hybrid microgels with variable ZnS contents have been prepared. It has been found that the hybrid particles possess both thermosensitive properties of VCL/AAEM matrix and typical physicochemical properties of bulk ZnS. Obtained hybrid microgels are quite stable in aqueous solution, but increase of ZnS content increases the sedimentation velocity of particles. Light scattering measurements indicate that hybrid microgels are also sensitive to pH due to the presence of inorganic particles in their structure which change their charge with respect to the pH value of the aqueous solution. Obtain hybrid microgels can form organized arrays on different substrates during drying process, and this self-assembly process can be easily controlled by adjusting the temperature or pH. This interesting feature can be used for preparation of patterned surfaces on nanoscale and useful for numerous applications.

Acknowledgment. The authors are thankful to Mrs. E. Kern for SEM measurements, Mrs. I. Poitz for TGA investigations, and Deutsche Forschungsgemeinschaft (DFG) with collaboration research project SFB 287 “Reactive Polymers” for financial support.

References and Notes

(1) Kawaguchi, H. *Prog. Polym. Sci.* **2000**, *25*, 1171.
(2) Bergbreiter, D. E.; Case, B. L.; Liu, Y. S.; Caraway, J. W. *Macromolecules* **1998**, *31*, 6053.
(3) Justin, D.; Debord, L.; Lyon, A. *J. Phys. Chem. B* **2000**, *104*, 6327.
(4) Hong, M.-Y.; Yoon, H. C.; Kim, H.-S. *Langmuir* **2003**, *19*, 4866.
(5) Narita, M.; Nomura, R.; Tomita, I.; Endo, T. *Macromolecules* **2000**, *33*, 4979.
(6) Zhang, J.; Xu, S.; Kumacheva, E. *J. Am. Chem. Soc.* **2004**, *126*, 7908.
(7) Scholz, S. M.; Vacassy, R.; Dutta, J.; Hofmann, H.; Akinc, M. *J. Appl. Phys.* **1998**, *83*, 7860.
(8) Yamaguchi, T.; Yamamoto, Y.; Tanaka, T.; Yoshida, A. *Thin Solid Films* **1999**, *344*, 516.
(9) Harris, D. C. *Infrared Phys. Technol.* **1998**, *39*, 185.
(10) Wilhelmy, D. M.; Matijevic, E. *J. Chem. Soc., Faraday Trans.* **1984**, *80*, 563.
(11) Williams, R.; Yocom, P. N.; Sofko, F. S. *J. Colloid Interface Sci.* **1985**, *106*, 388.
(12) Rana, R. K.; Zhang, L.; Yu, J. C.; Mastai, Y.; Gedanken, A. *Langmuir* **2003**, *19*, 5904.
(13) Xia, B.; Lenggoro, W.; Okuyama, K. *Chem. Mater.* **2002**, *14*, 4969.
(14) Chen, W.; Joly, A. G.; Malm, J.-O.; Bovin, J.-O.; Wang, S. *J. Phys. Chem. B* **2003**, *107*, 6544.
(15) Denzler, D.; Olschewski, M.; Sattler, K. *J. Appl. Phys.* **1998**, *84*, 2841.
(16) Scholz, S. M.; Vacassy, R.; Dutta, J.; Hofmann, H. *J. Appl. Phys.* **1998**, *83*, 7860.
(17) Vogel, W. *Langmuir* **2000**, *16*, 2032.

(18) Yanagida, S.; Ishimaru, Y.; Miyake, I.; Shiragami, T.; Pac, C.; Hashimoto, K.; Tadayoshi, S. *J. Phys. Chem.* **1989**, *93*, 2576.
(19) Bai, C.; Fang, Y.; Zhang, Y.; Chen, B. *Langmuir* **2004**, *20*, 263.
(20) Velikov, K. P.; Blaaderen, A. *Langmuir* **2001**, *17*, 4779.
(21) Breen, M. L.; Dinsmore, A. D.; Pink, R. H.; Qadri, S. B.; Ratna, B. R. *Langmuir* **2001**, *17*, 903.
(22) Sobisch, T.; Lerche, D. *Colloid Polym. Sci.* **2000**, *278*, 369.
(23) Killmann, E.; Eisenlauer, J. *Prog. Colloid Polym. Sci.* **1976**, *60*, 147.
(24) Wilhelmy, D. M.; Matijevic, E. *J. Chem. Soc., Faraday Trans.* **1984**, *180*, 563.
(25) Pich, A.; Bhattacharya, S.; Boyko, V.; Adler, H.-J. P. *Langmuir* **2004**, *20*, 10706.
(26) Boyko, V.; Pich, A.; Lu, Y.; Richter, S.; Arndt, K.-F.; Adler, H.-J. P. *Polymer* **2003**, *44*, 7821.
(27) Pich, A.; Lu, Y.; Boyko, V.; Arndt, K.-F.; Adler, H.-J. P. *Polymer* **2003**, *44*, 7651.
(28) Pich, A.; Lu, Y.; Boyko, V.; Arndt, K.-F.; Adler, H.-J. P. *Polymer* **2004**, *45*, 1079.
(29) Du, H.; Xu, Q.; Chin, W. S. *Chem. Mater.* **2002**, *14*, 4473.

MA0505272